19951213862

N95-27

Earth Horizon Modeling and Application to Static Earth Sensors on TRMM Spacecraft*

J. Keat and M. Challa
Computer Sciences Corporation (CSC)
Lanham-Seabrook, Maryland, USA

D. Tracewell and K. Galal
Goddard Space Flight Center (GSFC)
Greenbelt, Maryland, USA

Abstract

Data from Earth sensor assemblies (ESAs) often are used in the attitude determination (AD) for both spinning and Earth-pointing spacecraft. The ESAs on previous such spacecraft for which the ground-based AD operation was performed by the Flight Dynamics Division (FDD) used the Earth scanning method. AD on such spacecraft requires a model of the shape of the Earth disk as seen from the spacecraft. AD accuracy requirements often are too severe to permit Earth oblateness to be ignored when modeling disk shape. Section 2 of this paper rexamines and extends the methods for Earth disk shape modeling employed in AD work at FDD for the past decade. A new formulation, based on a more convenient Earth flatness parameter, is introduced, and the geometric concepts are examined in detail. It is shown that the Earth disk can be approximated as an ellipse in AD computations.

Algorithms for introducing Earth oblateness into the AD process for spacecraft carrying scanning ESAs have been developed at FDD and implemented into the support systems. The Tropical Rainfall Measurement Mission (TRMM) will be the first spacecraft with AD operation performed at FDD that uses a different type of ESA—namely, a static one—containing four fixed detectors D_i (i = 1 to 4). Section 3 of this paper considers the effect of Earth oblateness on AD accuracy for TRMM. This effect ideally will not induce AD errors on TRMM when data from all four D_i are present. When data from only two or three D_i are available, however, a spherical Earth approximation can introduce errors of 0.05 degrees to 0.30 degrees on TRMM. These oblateness-induced errors are eliminated by a new algorithm that uses the results of Section 2 to model the Earth disk as an ellipse.

1. Introduction

Data from Earth sensor assemblies (ESAs) often are used in attitude determination (AD) for both spinning and Earth-pointing spacecraft. Past spacecraft with AD operations performed at the Flight Dynamics Division (FDD) used Earth scanning ESAs. The Tropical Rainfall Measurement Mission (TRMM) will be the first such spacecraft to use a different type of ESA—namely, a static Earth sensor assembly (SESA), built by Barnes Engineering Company, that comprises four detectors D_i (i = 1 to 4) to sense the Earth horizon at four equally spaced points.

AD algorithms that use ESA data require a model of the shape of the Earth disk as seen from the spacecraft. Frequently, AD accuracy requirements are too severe to permit the simple approximation that the Earth is a sphere, yielding a perfectly circular disk. In such cases, a more exact disk shape model, which includes the effect of Earth oblateness, is needed. The methodology prescribed by Liu[1] has provided the basis for Earth oblateness and disk shape modeling at FDD since the late 1970s.

Techniques for including Earth oblateness in AD and for correcting attitudes in which it has not been included, on either spinning or Earth-pointing spacecraft using scanning ESAs, have been used at FDD for many years[2,3,4]. No analogous techniques were available previously at FDD for spacecraft that carry the Barnes SESA. As discussed later, such spacecraft do not require a correction for Earth oblateness in AD if the spacecraft, like TRMM, is nominally oriented along the geodetic nadir or horizon bisector nadir (rather than along the geocentric nadir) and if data from all four D_i are available. However, conditions in which data from only two or three of the four D_i are present are not infrequent. While attitude (roll and pitch angles) can be computed with data from only two or three adjacent D_i, the simple AD algorithms previously used in these cases permit Earth oblateness-induced AD errors.

---

* This work was supported by the National Aeronautics and Space Administration (NASA)/Goddard Space Flight Center (GSFC), Greenbelt, Maryland, Contract NAS 5-31500.

PRECEDING PAGE BLANK NOT FILMED

This paper is divided into two subsequent sections. In Section 2, Liu's Earth disk shape analysis is re-examined and extended, and some of the concepts are explored in more detail. The structure of Section 2 largely follows that of Reference 1, and some of the material presented in Section 2 has appeared earlier in References 5 and 6. In Section 3, a new AD algorithm is prescribed for TRMM when data from only three or two D_i are present.

2. Earth Horizon Modeling

2.1 The Earth Spheroid (ES)

Previous AD work at FDD involving nonspherical Earth modeling approximated the Earth as an oblate spheroid prescribed as follows:

$$x^2 + y^2 + z^2[1-f]^{-2} = a^2 \tag{1}$$

where a is the equatorial radius, and f is the flattening. The figure specified by Eq. (1) is called the Earth spheroid (ES) here. It was noted recently by Challa[5], however, that using a different flattening parameter α related to f as follows

$$\alpha = -1 + (1-f)^{-2} \tag{2}$$

is convenient because it facilitates the use of vector methods. Assuming f = 1/298.257, Eq. (2) yields α = 1/148.379; thus the Earth's α is approximately $2f$.

Eq. (2) enables Eq. (1) to be written as

$$\vec{r} \bullet \vec{r} + \alpha[\vec{r} \bullet \hat{z}]^2 = a^2 \tag{3}$$

where $\hat{z}$ is a unit vector from the geocenter, O, along the North pole axis, and $\vec{r}$ is the geocentric radius vector to an arbitrary point on the ES.

We view Eq. (3) as a constraint on $\vec{r}$, which we call the *ES constraint*. Our immediate goal is to define, on the ES, the Earth horizon contour as seen from a spacecraft, S. This requires specifying one more constraint on $\vec{r}$, and this topic is addressed in the following sections (2.2 and 2.3).

2.2 The Horizon Spheroid (HS)

Define the following scalar field

$$f(\vec{r}) = \vec{r} \bullet \vec{r} + \alpha[\vec{r} \bullet \hat{z}]^2 \tag{4}$$

and let $\vec{g}(\vec{r})$ be its gradient

$$\vec{g}(\vec{r}) = 2\left[\vec{r} + \alpha\,(\vec{r} \bullet \hat{z})\,\hat{z}\right] \tag{5}$$

We view Eq. (4) as specifying an infinite family of oblate spheroids, each with constant equatorial radius sqrt $\left(f(\vec{r})\right)$ and all elements of the family having flattening α and center at O. Let $E(\vec{r})$ denote the spheroid at the tip of $\vec{r}$ and let $T(\vec{r})$ be the tangent plane to $E(\vec{r})$ at $\vec{r}$. Then $\vec{g}(\vec{r})$ is orthogonal to $T(\vec{r})$.

Let $\vec{s}$ be a vector from O to a spacecraft, S. Let $\vec{h}(\vec{r})$ be a vector from S to $\vec{r}$. Obviously,

$$\vec{h}(\vec{r}) = \vec{r} - \vec{s} \tag{6}$$

Our second constraint on $\vec{r}$ is that S, and hence $\vec{h}(\vec{r})$, lie in $T(\vec{r})$. Then,

$$\vec{h}(\vec{r}) \bullet \vec{g}(\vec{r}) = 0 \tag{7}$$

Eq. (7) is the first form of the second constraint on $\vec{r}$. Satisfaction of this constraint implies that the tip of $\vec{r}$ is a horizon point of $E(\vec{r})$. A more explicit form of Eq. (7) can be obtained by introducing Eqs. (5) and (6) into it to produce

$$\vec{r} \bullet \left[\vec{r} - \vec{s}\right] + \alpha \left[\vec{r} \bullet \hat{z}\right]\left[\hat{z} \bullet \left(\vec{r} - \vec{s}\right)\right] = 0 \tag{8}$$

To transform Eq. (8) into a form that clearly shows the shape of the figure defined by the second constraint, add $\left(\vec{s}/2\right) \bullet \left(\vec{s}/2\right)$ to both sides and factor. For simplicity, then introduce $\vec{v} = \vec{r} - \vec{s}/2$. The result is

$$\vec{v} \bullet \vec{v} + \alpha \left[\vec{v} \bullet \hat{z}\right]^2 = \frac{\vec{s}}{2} \bullet \frac{\vec{s}}{2} + \alpha \left[\hat{z} \bullet \frac{\vec{s}}{2}\right]^2 \tag{9}$$

Eq. (9) shows that the second constraint requires the tip of $\vec{r}$ to lie on an oblate spheroid, called the horizon spheroid (HS) here. Similarly, we call the second constraint the horizon spheroid constraint. The HS is centered at $\vec{s}/2$ and, like the ES, has flattening α. The equatorial plane of the HS is parallel to that of the ES, and its equatorial radius is the square root of the term on the right side of Eq. (9). Points O and S both lie on the HS.

2.3 The Horizon Plane (HP)

Eqs. (3) and (8) constitute a pair of constraints on $\vec{r}$ which, when solved for $\vec{r}$, define a closed curve, called here the *horizon contour* (HC), which is the ES horizon seen from S and specified on the ES. Geometrically, the HC is the intersection of two oblate spheroids; namely, the ES and HS, as illustrated in Fig. 1.

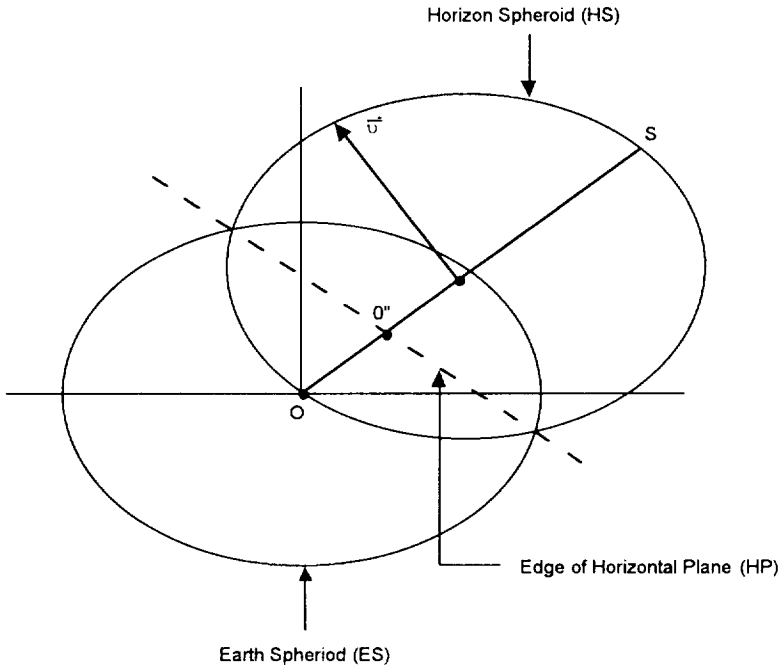

Figure 1. Earth Spheroid, Horizon Spheroid, and Horizon Plane

The geometry and the solution for $\vec{r}$, however, can be simplified by replacing the HS constraint by a new constraint formed from the ES and HS ones. To develop this new constraint, first note that Eqs. (4) and (5) show that $\vec{r} \bullet \vec{g}\left(\vec{r}\right) = 2f\left(\vec{r}\right)$ and Eqs. (6) and (7) indicate $\vec{r} \bullet \vec{g}\left(\vec{r}\right) = \vec{s} \bullet \vec{g}\left(\vec{r}\right)$. Hence

$$\vec{s} \bullet \vec{g}\left(\vec{r}\right) = 2f\left(\vec{r}\right) \tag{10}$$

Eq. (10) is merely another form of the HS constraint. Eqs. (3) and (4) show that the ES constraint can be written as merely

$$f\left(\vec{r}\right) = a^2 \tag{11}$$

The initial equation for the new constraint is produced by inserting Eq. (11) into Eq. (10) to obtain trivially

$$\vec{s} \bullet \vec{g}(\vec{r}) = 2a^2 \tag{12}$$

For a more useful form of the new constraint, first introduce Eq. (5) into Eq. (12) and manipulate to obtain

$$\vec{m} \bullet \vec{r} = a^2 \tag{13}$$

where

$$\vec{m} = s\left[\hat{s} + \alpha\hat{z}\cos\lambda'\right] \tag{14}$$

In Eq. (14) we have factored $\vec{s}$ into $\vec{s} = s\hat{s}$ and introduced λ' as the co-latitude angle between $\hat{s}$ and $\hat{z}$. Using $\vec{m} = m\hat{m}$, Eq. (14) indicates that

$$m = s\left[1 + 2\alpha\left(1 + 0.5\alpha\right)\cos^2\lambda'\right]^{1/2} \tag{15}$$

Define the following vector $\vec{n}$ along $\hat{m}$:

$$\vec{n} = n\hat{m} \tag{16}$$

where

$$n = a^2/m \tag{17}$$

Eq. (13) then can be written as

$$\vec{r} \bullet \hat{m} = n \tag{18}$$

Eq. (18) is the second form of the new constraint. Analysis of Eq. (18) shows it constrains the tip of $\vec{r}$ to lie on a plane whose normal is along $\hat{m}$ and whose distance from O is n. This plane and the new constraint are called the *horizon plane* (HP) and HP constraint here. An alternate derivation of Eq. (18) is presented in Ref. 5.

Some later-needed properties of the HP will be delineated before proceeding. Fig. 2 shows the geometry. With the exception of $\hat{E}$, all vectors on this figure lie in a plane normal to the HP. O' is the tip of the perpendicular from O to the HP, and O'' is the intersection of $\vec{s}$ with the HP. The position vectors of O' and O'' with respect to O are given by $\vec{n}$ and $s_1\hat{s}$, respectively. The distance between O'' and S is given by s_2; thus, $s_1 + s_2 = s$. The term b is the distance between O' and O''. The unit vectors $\hat{E}$ and $\hat{N}$ are directed along local East and local North, respectively, at O' and define the HP. The triad ($\hat{E}$, $\hat{N}$, $\hat{m}$) defines a reference frame centered at O'. The vector $\hat{m}$ makes angles σ and ε_m with $\hat{z}$ and $\hat{s}$, respectively. Note that ε_m is a small angle, since the ES is very nearly spherical; the size of ε_m has been exaggerated on Fig. 2 for clarity.

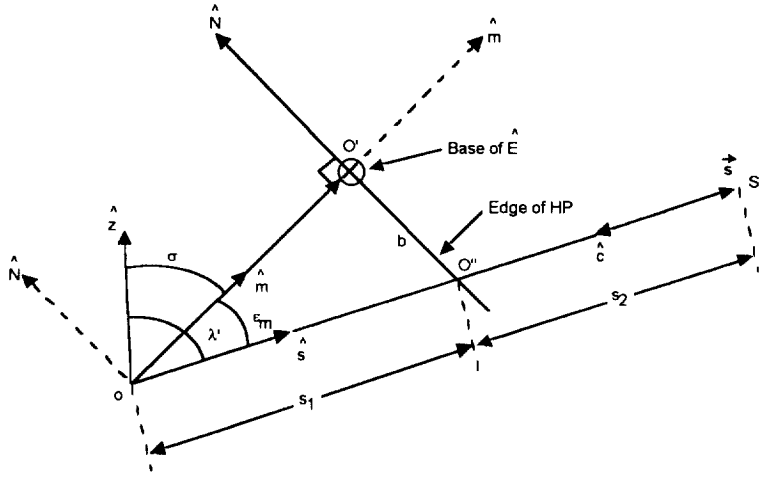

Figure 2. Horizon Plane Geometry and Variables

The following important relations can be derived using the material presented above:

$$\cos\sigma = \hat{m} \bullet \hat{z} = \left[s/m\right]\left[1+\alpha\right]\cos\lambda' \tag{19}$$

$$\sin\sigma = \left[s/m\right]\sin\lambda' \tag{20}$$

$$\cos\varepsilon_m = \hat{s} \bullet \hat{m} = \left[s/m\right]\left[1+\alpha\cos^2\lambda'\right] \tag{21}$$

$$\sin\varepsilon_m = \left[s/m\right]\alpha\sin\lambda'\cos\lambda' \tag{22}$$

$$\hat{E} = \hat{z} \times \hat{s}/\sin\lambda' \tag{23}$$

$$\hat{N} = \hat{m} \times \hat{E} = \left[s/\left(m\sin\lambda'\right)\right]\left[\hat{z}\left(1+\alpha\cos^2\lambda'\right) - \hat{s}\left(1+\alpha\right)\cos\lambda'\right] \tag{24}$$

$$b = \left[\alpha a^2/m\right]\cos\lambda'\sin\lambda'\left[1+\alpha\cos^2\lambda'\right]^{-1} \tag{25}$$

$$s_1 = \left[a^2/s\right]\left[1+\alpha\cos^2\lambda'\right]^{-1} \tag{26}$$

$$s_2 = s\left[1+\alpha\cos^2\lambda' - \left(a/s\right)^2\right]\left[1+\alpha\cos^2\lambda'\right]^{-1} \tag{27}$$

Note that Eqs. (21) and (15) yield

$$\cos\varepsilon_m \approx 1 - \frac{\alpha^2\sin^2\lambda'\cos^2\lambda'}{2} \tag{28}$$

Thus, the angle between $\hat{s}$ and $\hat{m}$ is given by

$$\varepsilon_m \approx \alpha\sin\lambda'\cos\lambda' \tag{29}$$

except for the cases $\lambda' = 0$ and $\lambda' = \pi/2$. Thus, the geocenter-to-spacecraft vector $\vec{s}$ generally differs from the normal to the HP by an angle of the order of the flattening factor α.

It will be shown in Section 2.4 that the locus of the horizon points in the HP is an ellipse, and it will then be shown that the spacecraft views this ellipse slightly obliquely.

2.4 The Horizon Ellipse (HE)

The HC now is specified by Eqs. (3) and (18) as the intersection of a spheroid and a plane; namely, the ES and the HP, as illustrated in Fig 1. To solve these equations, express $\vec{r}$ as

$$\vec{r} = \vec{n} + \vec{w} \tag{30}$$

with $\vec{w} \bullet \vec{n} = 0$. Thus, $\vec{w}$ lies in the HP, with its base at O'. Eq. (30) thus requires $\vec{r}$ to satisfy the HP constraint. To further restrict $\vec{r}$ to satisfy the ES constraint, insert Eq. (30) into Eq. (3). After manipulation, we obtain

$$\vec{w} \bullet \vec{w} + \alpha\left[\vec{w} \bullet \hat{z}\right]^2 + 2\alpha\left[\vec{n} \bullet \hat{z}\right]\left[\vec{w} \bullet \hat{z}\right] = a^2 - \vec{n} \bullet \vec{n} - \alpha\left[\vec{n} \bullet \hat{z}\right]^2 \tag{31}$$

Eq. (31), in conjunction with Eq. (30), specifies the HC.

Eq. (31) can be transformed into a simpler form by specifying the position vector of the horizon point relative to O'' rather than relative to O'. Letting $\vec{q}$ be this new position vector and noting that $\overrightarrow{O''O'} = b\hat{N}$ as is evident from Fig. 2, we thus have

$$\vec{w} = \vec{q} - \hat{N}b \tag{32}$$

with $\vec{q}$, like $\vec{w}$, restricted to the HP.

When Eq. (32) is inserted into Eq. (31), it can be shown, with much work, that a pair of terms cancel out, yielding the following simpler result:

$$\vec{q} \bullet \vec{q} + \alpha_E \left[\hat{N} \bullet \vec{q}\right]^2 = a^2{}_E \tag{33}$$

where

$$\alpha_E = \alpha\left[\hat{N} \bullet \hat{z}\right]^2 = \alpha[s/m]^2 \sin^2 \lambda' \tag{34}$$

$$\begin{aligned} a^2{}_E &= a^2 - \vec{n} \bullet \vec{n} - \alpha[\vec{n} \bullet \hat{z}]^2 \left[1 + \alpha\left(\hat{N} \bullet \hat{z}\right)^2\right]^{-1} \\ &= a^2\left[1 + \alpha \cos^2 \lambda' - (a/s)^2\right]\left[1 + \alpha \cos^2 \lambda'\right]^{-1} \end{aligned} \tag{35}$$

Eq. (33) shows that the shape of the HC in the HP is an ellipse, called the *horizon ellipse* (HE) here. The center of the HE is at O'', its flattening is α_E and its semi-major axis is a_E along $\hat{E}$. The HC's elliptical shape and the important fact that its center is on $\vec{s}$ were noted in Ref. 5.

2.5 The Earth Disk (ED)

We use the term *Earth disk* (ED) here to denote the figure of the Earth as seen from S. The next task is to specify the ED's shape from the preceding material on the HP and HE. Fig. 3 shows the geometry.

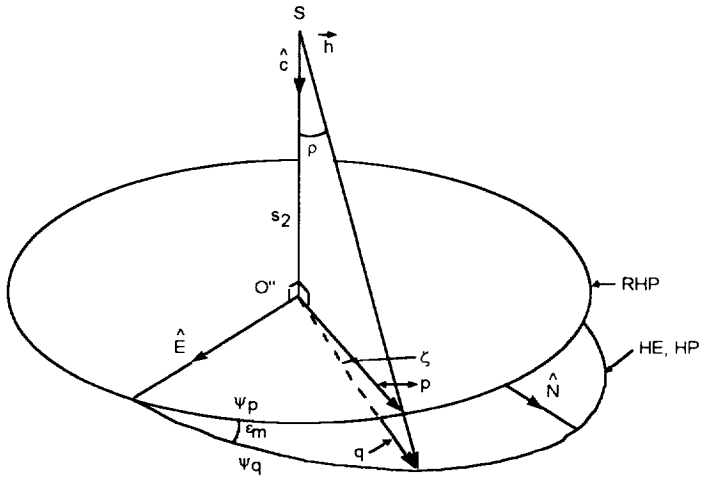

Figure 3. Earth Angular Radius ρ Geometry

The previous section (2.4) showed that the HP is not quite orthogonal to $\vec{s}$. So we will define a new plane, called here the *rotated horizon plane* (RHP), which is orthogonal to $\vec{s}$. The RHP is formed by rotating the HP about $\hat{E}$ through angle ε_m. Let $\vec{q} = q\hat{q}$ be a vector on the HE at an azimuth angle ψ_q from $\hat{E}$. Let $\vec{p} = p\hat{p}$ be the vector in the RHP corresponding to $\vec{q}$. Let ψ_p be the azimuth angle of $\vec{p}$ from $\hat{E}$. $\vec{p}$ is formed by projecting $\vec{q}$ along the vector $\vec{h}$ onto the RHP, where $\vec{h}$ is the horizon vector from S to the tip of $\vec{q}$. Obviously, the locus $\vec{p}\left(\psi_p\right)$ in the RHP is not an ellipse centered at O''. Designate the small angle between $\vec{p}$ and $\vec{q}$ as ζ. The following important equations can be derived:

$$p = q \cos\zeta \left[1 + \left(q/s_2\right)\sin\zeta\right]^{-1} \tag{36}$$

$$\sin\zeta = \sin\psi_q \sin\varepsilon_m \tag{37}$$

$$\cos\zeta = c_1 \cos\varepsilon_m \tag{38}$$

$$\sin\psi_q = c_1 \sin\psi_p \tag{39}$$

$$\cos\psi_q = c_1 \cos\varepsilon_m \cos\psi_p \tag{40}$$

$$c_1 = \left[1 - \sin^2 \varepsilon_m \cos^2 \psi_p\right]^{-0.5} \tag{41}$$

$$q = a_E\left[1 + \alpha_E \sin^2 \psi_q\right]^{-0.5} \tag{42}$$

Let ρ be the angle at S between $\vec{h}$ and the unit geocentric nadir vector $\hat{c} = -\hat{s}$. The shape of the ED will be specified by the locus of $\rho(\psi_p)$ around it. It turns out that the simplest result is obtained using the arcctn function:

$$\rho = \text{arcctn}(s_2/p) \tag{43}$$

Insert Eq. (36) into Eq. (43), and use Eqs. (37) through (42) and earlier equations as necessary. After much work, the following important result ensues:

$$\rho = \text{arcctn}\left\{\left[1 + \alpha\cos^2\lambda'\right]^{-1}\left[\alpha\sin\lambda'\cos\lambda'\sin\psi_p + \text{ctn}\,\rho_c\left[1 + \alpha\left(k_1 + k_2\sin^2\psi_p\right)\right]^{0.5}\right]\right\} \tag{44a}$$

where

$$k_1 = \cos^2\lambda'\left[1 + \sec^2\rho_c\left(1 + \alpha\cos^2\lambda'\right)\right] \tag{44b}$$

$$k_2 = \sin^2\lambda'\left[1 + \alpha\cos^2\lambda'\sec^2\rho_c\right] \tag{44c}$$

$$\rho_c = \arcsin(a/s) \tag{45}$$

ρ_c above is merely the usual angular radius, from S, of a fictitious spherical Earth with radius a and center at O.

Eqs.(44a) through (44c) were derived earlier in Ref. 6 using a different approach. Ref. 6 shows, by analytical and numerical means, that Eqs. (44a) through (44c) are equivalent to Eq. (4-24) of Ref. 1.

2.6 The Earth Disk Ellipse Approximation

The Earth's α is small enough to permit Eqs. (44a) through (44c) to be linearized in it with acceptable accuracy. The result is

$$\text{ctn}\,\rho = \text{ctn}\,\rho_c\left[1 + 0.5\alpha\left\{\cos^2\lambda'\sec^2\rho_c\sin^2\rho_c + 2\sin\lambda'\cos\lambda'\tan\rho_c\sin\psi_p + \sin^2\lambda'\sin^2\psi_p\right\}\right] \tag{46}$$

Eqs. (44) and (46) specify disk angular radius ρ relative to the geocentric nadir z_c. We wish to generalize Eq. (46) to specify disk radius relative to lines close to z_c. Fig. 4 shows the geometry on the unit celestial sphere (UCS). Point P here lies on the extension of z_c onto the UCS. The reference origin is to be moved from P south through small angle ε to a new point P_ε by transforming Eq. (46) from variables ρ, ψ_p to new ones ρ_ε, ψ_ϵ. For now, ε is assumed to be arbitrary, but small enough to permit small angle approximations and ruthless linearizations. Fig. 4 then yields

$$\text{ctn}\,\rho = \text{ctn}\,\rho_\varepsilon\left[1 + \varepsilon\sec\rho_\varepsilon\csc\rho_\varepsilon\sin\psi_\varepsilon\right] \tag{47}$$

$$\sin^2\psi_p = \sin^2\psi_\varepsilon\left[1 - 2\,\varepsilon\,\text{ctn}\,\rho_\varepsilon\cos^2\psi_\varepsilon\csc\psi_\varepsilon\right] \tag{48}$$

$$\sin\psi_p = \sin\psi_\varepsilon\left[1 - \varepsilon\,\text{ctn}\,\rho_\varepsilon\cos^2\psi_\varepsilon\csc\psi_\varepsilon\right] \tag{49}$$

Insert Eqs. (48) and (49) into Eq. (46) and equate to Eq. (47). This produces an equation in the desired terms ε, ρ_ε, ψ_ε. However, it is not evident how to solve it for ρ_ε in closed form.

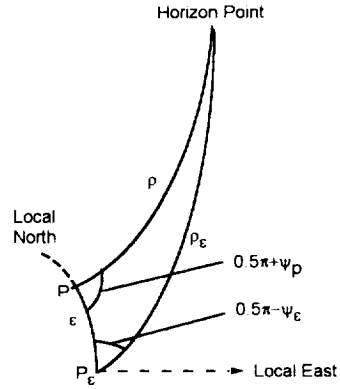

Figure 4. Origin Translation on Unit Celestial Sphere (UCS)

The difficulty will be handled by now restricting the work to a single, highly important case. Specifically, ε now will be limited to the value that causes the two terms involving itself and sin ψ_ε, respectively to cancel. The subscript *HB*, for *horizon bisector*, will be used to denote this ε and terms pertaining to it. The resulting equation for ε_{HB} is

$$\varepsilon_{HB} = \alpha \cos\lambda' \sin\lambda' \sin^2 \rho_c \tag{50}$$

It should be realized that ε_{HB} is the angle between z_c and a line, z_{HB}, called here the *horizon bisector nadir*. An alternate name, the *apparent nadir*, has been used by Flatley[7] who performed the original work on the concept. The resulting equation for $\text{ctn}\,\rho_{HB}$ when Eq. (50) is used is

$$\text{ctn}\,\rho_{HB} = \text{ctn}\,\rho_c \left[1 + 0.5\alpha \left\{\cos^2 \lambda' \sec^2 \rho_c \sin^2 \rho_c + \sin^2 \lambda' \sin^2 \psi_{HB}\right\}\right] \tag{51}$$

Solving Eq. (51) for ρ_{HB} and linearizing in α produces

$$\rho_{HB} = a_E \left[1 - 0.5\alpha_E \sin^2 \psi_{HB}\right] \tag{52a}$$

where

$$a_E = \rho_c - 0.5\alpha \cos^2 \lambda' \sin^3 \rho_c \sec \rho_c \tag{52b}$$

$$\alpha_E = 0.5(\alpha/\rho_c) \sin\rho_c \cos\rho_c \sin^2 \lambda' \tag{52c}$$

Eqs. (52a) through (52c) show that the ED can be approximated by an ellipse, centered at ρ_{HB} with flattening α_E and semi-major axis a_E along local East. This result was derived earlier in Ref. 6 by different means. A MATLAB study, described in Ref. 6, indicated that for the Earth α, the ellipse approximation is accurate to about 1e-5 degrees. It should be realized, however, that the ellipse exists only on an abstract mathematical plane, not on a physical one. Geometrically, the figure of the Earth seen from S can, of course, best be considered to exist on the UCS, not on a plane.

3. Application to TRMM Attitude Determination

3.1 Introduction

Fig. 5 shows the nominal TRMM SESA FOV geometry on a circular ED. The basic outputs of the SESA are the four positive penetration angles X_i between the Earth IR horizon and the detector D_i bases. Spacecraft attitude is specified by a 2 × 1 vector $\underline{\beta}$ of the angular deviation of the SESA and spacecraft body axis $z_S = z_B$ from the HB nadir line z_{HB}. There are two main steps in the AD process. First, the X_i are transformed into an SESA frame, *S*, attitude vector $\underline{\beta}_S = \left[\phi_S \theta_S\right]^T$ using the

algorithms discussed below. Second, $\underline{\beta}_S$ is transformed into a spacecraft body, B, frame vector $\underline{\beta}_B = [\phi_B \theta_B]^T$ by a rotation $\underline{\beta}_B = R\underline{\beta}_S$. Our current interest is only in the first of these two operations. The ϕ and θ are roll and pitch angles; determination of yaw is done separately and requires a separate sensor.

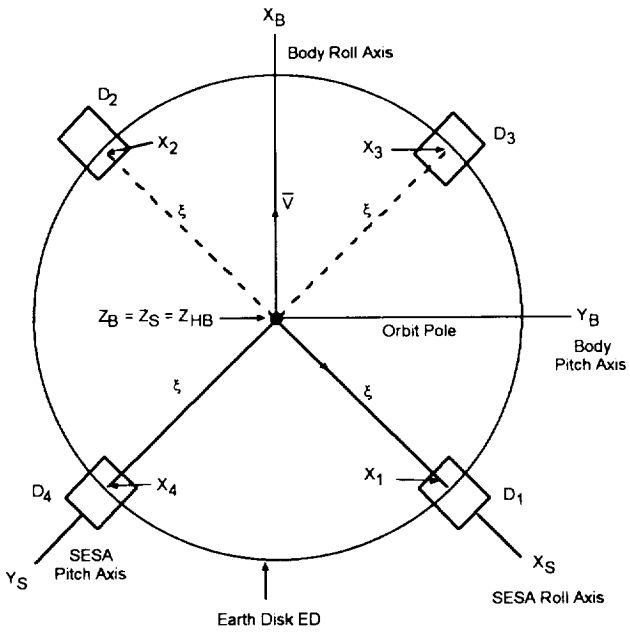

Figure 5. Nominal SESA FOV Geometry on Earth Disk (ED)

3.2 The Standard SESA AD Algorithms

The standard algorithms for computing $\underline{\beta}_S$ from the X_i imply a spherical model of the Earth. When all four X_i are available, we use

$$\phi_S = 0.5[X_4 - X_3] \tag{53}$$

$$\theta_S = 0.5[X_2 - X_1] \tag{54}$$

If only three X_i are available, either Eq. (53) or Eq. (54) will be unusable, requiring a new algorithm for the affected angle. For example, if X_3 is missing, then ϕ_S is computed via

$$\phi_S = X_4 - 0.5[X_1 + X_2] \tag{55}$$

and if X_1 is missing, θ_S is computed via

$$\theta_S = X_2 - 0.5[X_3 + X_4] \tag{56}$$

Analogous algorithms are used when X_2 or X_4 is missing. The function of the final terms in Eqs. (55) and (56) is to compensate for deviation of altitude from that which yields all $X_i = 0$ in the nominal spherical Earth attitude condition.

When the X_i from two adjacent D_i, say D_1 and D_3, are missing, we use

$$\phi_S = X_4 - X_{AVG} \tag{57}$$

$$\theta_S = X_2 - X_{AVG} \tag{58}$$

with

$$X_{AVG} = X_R - \alpha_R \left[h - h_R\right] \tag{59}$$

where h is actual altitude, h_R is a reference altitude, X_R is the nominal spherical Earth X_i at h_R, and α_R is a scale factor.

3.3 Proposed AD Algorithms to Compensate for Earth Oblateness

Section 2.6 demonstrated that to first order in α, the ED is an ellipse with center P_{HB} on z_{HB}. Therefore, due to symmetry, Earth oblateness will not introduce an error into the attitude computed by Eqs. (53) and (54). Numerical studies using the software package MATLAB showed that, in fact, this result does not depend on the first order approximation in α. Thus, Earth oblateness does not induce an AD error when all four X_i are available and used.

Our MATLAB studies, however, also showed that Earth oblateness induces a significant AD error on TRMM when only three or two X_i are available and Eqs. (55) through (59) are used. This error varies from 0 to 0.05 degrees in the $3-X_i$ case and from 0.05 to 0.30 in the $2-X_i$ one. To eliminate the AD errors in the $3-X_i$ and $2-X_i$ cases, we have proposed that Eqs. (55) through (59) be replaced by a new algorithm based on the elliptical ED model from Section 2.6. The main steps of this algorithm are as follows.

(1) Compute the azimuth angles ψ_{D_i} of the D_i relative to local East via

$$\psi_{D_i} = \psi - \psi_v - \psi_{D_iB} \tag{60}$$

where ψ is the spacecraft yaw angle, ψ_{D_iB} is the constant azimuth angle of each D_i relative to x_B, and ψ_v is the spacecraft velocity angle relative to local East. ψ_v can be computed using

$$\psi_v = \pi/2 - \arctan\left(\cos i/\cos\left(\omega + f\right)\right) \tag{61}$$

where i, ω, and f are orbit inclination, argument of perigee, and true anomaly, respectively.

(2) Use the ψ_{D_i} to compute the ED radii ρ_{D_i} at the D_i using Eq. (52). Then compute the nominal penetration angles X_{iNOM} via $X_{iNOM} = \psi_{D_i} - \xi$; where ξ is the detector mounting angle on Fig. 5.

(3) Compute the ϕ_S and/or θ_S that cannot be computed by Eq. (53) and/or Eq. (54) via

$$\phi_S = X_i - X_{iNOM} \tag{62}$$

$$\theta_S = X_j - X_{iNOM} \tag{63}$$

where X_i and X_j are the proper available penetration angles. Theory indicates this algorithm should almost perfectly eliminate Earth oblateness-induced AD errors in the $2-X_i$ and $3-X_i$ cases.

Acknowledgments

The authors acknowledge the considerable contributions to this paper by K. Liu through innumerable discussions and provision of his original derivations for Ref. 1.

References

1. Liu, K., "Earth Oblateness Modeling," in *Spacecraft Attitude Determination and Control,* J. Wertz, editor, D. Reidel, Dordrecht, Holland, 1978

2. Nair, G., et al., *Earth Radiation Budget Satellite (ERBS) Ground Support System (AGSS) Functional Specification and Requirements,* Computer Sciences Corporation,CSC/SD-82/6013, September 1982

3. Goddard Space Flight Center, Flight Dynamics Division, 553-FDD-93/032R1UD0, *Multimission Three-Axis Stabilized Spacecraft (MTASS) Flight Dynamics Support System (FDSS) Mathematical Background,* prepared by Computer Sciences Corporation, June 1994

4. Ottenstein, N., et al., *Multimission Spin-Axis Support System (MSASS) Functional Specification Revision 1,* Computer Sciences Corporation, 554-FDD-90/085R1UDO, prepared for Goddard Space Flight Center under Contract NAS 5-31500

5. Goddard Space Flight Center, Flight Dynamics Division 553-FDD-94/030R0UD0, *Attitude Determination Using Static Earth Sensors,* M. Challa, prepared by Computer Sciences Corporation, August 1994

6. Keat, J.E., "Shape of the Earth as Seen from Space," unpublished memo to Liu and Challa, September 1, 1994

7. Flatley, T.W., "TRMM Yaw," memo from 712.3/TRMM ACS lead analyst, D. McGlew, to Distribution, November 16, 1992

FLIGHT MECHANICS/ESTIMATION THEORY SYMPOSIUM

MAY 16-18, 1995

SESSION 4